

ANALYTICAL STUDY OF FRP CONFINED CONCRETE COLUMNS

by

Sohail Samdani¹ and Shamim A. Sheikh²

ABSTRACT

An analytical study was conducted on the behaviour of circular concrete columns confined with Fibre Reinforced Polymers (FRP). The data on FRP-confined columns from fourteen experimental investigations was compiled and critically examined to identify the variables that affect the behaviour of confined concrete. From the existing experimental data, twenty specimens were selected for the performance analysis of six existing analytical models. Results from the performance analysis showed that none of the existing models predicted the behaviour of FRP-confined columns with reasonable accuracy. Also, the models were unable to simulate the post-peak response exhibited by some of the specimens. A rational analytical model was developed to determine the complete stress-strain response of FRP-confined circular concrete columns. Predictions from this model were found to be reasonably accurate and a significant improvement over the existing models.

KEYWORDS

Columns, confinement, ductility, earthquake resistant structures, jacketing, FRP-confined concrete, strength.

ABOUT THE AUTHORS

¹ **Sohail Samdani** is currently working as a Structural Engineer in the Heavy Industrial Division of H. G. Engineering Ltd., Toronto, Ontario, Canada. He received his Bachelor of Civil Engineering degree in 2001 from the N.E.D. University of Engineering and Technology, Karachi, Pakistan, and his Master of Applied Science degree in 2003 from the University of Toronto, Ontario, Canada. His research interests include earthquake resistant design of structures and applications of FRP in concrete structures. Research reported in this paper is based on his Master's thesis research.

² **Shamim A. Sheikh**, *FACI*, is a professor of Civil Engineering at the University of Toronto, Canada. He is chair of joint ACI-ASCE Committee 441, Reinforced Concrete Columns and is a member of ACI Committee 374, Performance Based Seismic Design of Concrete Buildings. He is a fellow of American Concrete Institute and was the recipient of the ACI Structural Research Award in 1999. His research interests include earthquake resistance and seismic upgrade of concrete structures, confinement of concrete, use of FRP in concrete structures, expansive cement and its applications.

INTRODUCTION

It is widely accepted that columns failures can lead to total collapse of structures. Often, these columns are vulnerable to exceptional loads such as seismic, impact or explosion loads, etc. The structures may also be subjected to increased loads due to changes in serviceability requirements, or degradation as a result of corrosion of steel reinforcement, alkali silica reaction, etc. A change in design code may also render a structure deficient. Not only the strength but also the ductility needs to be enhanced in many cases to improve the structural performance particularly under seismic loads. Confinement of concrete has been proven to be an effective technique in increasing the ductility of the concrete members and to a lesser degree, in improving their strength.

The behaviour of confined concrete has been subjected to countless studies over the last century. It is generally accepted that when uniaxially loaded concrete is restrained from expanding laterally, it exhibits increased strength and axial deformation capacity. A large number of experimental and analytical investigations have been carried out to study the behaviour of concrete columns confined with steel spirals or hoops. While lateral steel can provide effective confinement to concrete, it can corrode over time. Corrosion is especially prevalent in North America where the extreme environmental conditions can be deleterious to reinforced concrete structures.

In recent years, the use of fibre reinforced polymers (FRP) for strengthening and/or rehabilitation of civil engineering structures has progressed at a rapid pace. These high performance materials, consisting of high strength synthetic fibres embedded in a polymeric matrix, have unique properties (high strength-to-weight ratio, good corrosion behaviour, electromagnetic neutrality etc.) which make them extremely attractive for use

in structural applications. FRPs are being used for flexural and shear strengthening of reinforced concrete structures, but probably one of their most attractive application is their use to achieve confinement in concrete columns. For this purpose FRPs can be used in the form of prefabricated tubes, wraps or filaments.

With the advancement in the field of fibre reinforced composite materials and their successful application as a strengthening and retrofitting material in structural engineering, engineers need design guidelines and reliable information regarding the behaviour of concrete structures reinforced with fibre reinforced polymers.

A considerable amount of experimental and analytical research has been conducted to study the behaviour of FRP-confined concrete columns^[2-17]. However, it is observed that most of the experimental studies involved small-scale specimens. Accordingly, the existing analytical models are calibrated for small-scale specimens' data. It is widely accepted that as the size of specimens differs, so do the observed results. Analytical models must be equally applicable to large-scale as well as small-scale specimens before they can be used to develop design guidelines for implementation in the field.

RESEARCH SIGNIFICANCE

Availability of reliable analytical models for predicting the behaviour of FRP-confined concrete will enhance the confidence level of engineers to use fibre reinforced composites in the construction industry. In the absence of reliable models, they may be forced to either avoid the use of FRP materials or incorporate high factors of safety, making composite construction less economical.

The current research is directed at the analytical modelling of the behaviour of circular FRP-confined concrete columns, subjected to concentric monotonic axial compression. The objectives of the current study were to: i) Perform an extensive review of the existing experimental and analytical investigations on the behaviour of FRP-confined circular concrete columns, ii) Critically examine the existing experimental data and identify significant variables and evaluate their effects on the behaviour of concrete specimens, iii) Conduct a performance analysis of existing analytical models developed for FRP-confined concrete columns, and if necessary, iv) Develop an analytical model to accurately simulate the complete response of FRP-confined concrete columns and evaluate its validity for the selected specimens representing a wide range of different parameters.

Data from fourteen experimental investigations including those carried out at the University of Toronto, were analyzed to identify the variables that affect behaviour of confined concrete. Twenty specimens were selected for the performance analysis of six existing analytical models. Since no existing analytical model performed in a satisfactory manner, a new analytical model was developed to simulate the mechanism of confinement of concrete with FRP.

EXPERIMENTAL BEHAVIOUR OF FRP CONFINED CONCRETE

Summary of Literature Review

An extensive review of the most relevant and applicable confinement studies and models ^[2-17] was conducted during this research ^[1]. Following is the summary of the

common conclusions regarding the behaviour of FRP-confined concrete found during the review.

- The confinement action applied by FRP on the concrete core is a passive phenomenon, that is, it arises as a result of the lateral expansion of concrete under uniaxial compression. As the axial strain increases, the corresponding lateral strain increases and the confining device (FRP) develops a tensile hoop stress, balanced by a uniform radial pressure which reacts against the concrete lateral expansion.
- Concrete is a restraint-sensitive material, rather than a pressure-sensitive material. The dilation tendency of concrete is one of the most important factors in developing models for predicting the stress-strain behaviour of confined concrete.
- In general, the stress-strain responses reported in the literature (except for the tests conducted by Jaffry and Sheikh ^[2], and Cairns and Sheikh ^[3]) for FRP-confined concrete columns are bilinear with a sharp softening and a transition zone at approximately the level of corresponding unconfined concrete strength. The first linear zone solely depends on the concrete properties, the slope of stress-strain curve in this zone is same as the slope for unconfined concrete. As the stress level reaches near the unconfined concrete strength, the transition zone to the second portion of the bilinear curve starts. This region represents that the concrete has significantly cracked and the FRP tube has started to show its confining characteristics. The slope of the second branch of the stress-strain relationship is mainly related to the stiffness of the confining tube. The second linear branch continues until the peak stress is achieved at the point when FRP ruptures, resulting in the failure of the column.

- The confined concrete strength is essentially dependent on the maximum confining pressure that the FRP can apply, whereas the slope of the second branch of the stress-strain curve mainly depends on the stiffness of the FRP jacket.
- No post-peak response is reported in case of FRP-confined columns (except for the test conducted by Jaffry and Sheikh ^[2], and Cairns and Sheikh ^[3]). The peak point coincides with the ultimate point and both these points correspond to the tensile rupture of the FRP confining device.
- A number of researchers have reported that the strains measured in FRP at rupture are considerably lower than the ultimate strain of FRP tested in uniaxial coupon tests.
- The reported dilation response of FRP-confined concrete, like the axial stress-axial strain response, also consists of three regions. The initial rate of dilation is the same as the Poisson's ratio of unconfined concrete. The dilation rate remains constant during the initial stages of loading, when concrete behaves elastically. As severe micro-cracks begin to develop, the dilation rate starts to increase. For unconfined concrete, the dilation becomes unstable with further growth of cracks. However for FRP-confined concrete, the dilation rate reaches a maximum value, after which it stabilizes until the FRP ruptures. The maximum dilation ratio depends on the strength and stiffness of the FRP jacket and the concrete characteristics.
- The confinement models developed for concrete columns confined with steel tend to over predict the strength enhancement when applied to the FRP-confined concrete columns. This is mainly because of the behavioural difference between the two materials, that is steel and FRP. Steel, being an elasto-plastic material, exerts a constant confining pressure after its yield. While FRP, being a linearly elastic

material, confines the concrete with an ever-increasing confining pressure until its rupture. Moreover, these models do not incorporate the dilation tendency of confined concrete.

It should be noted here that most of the studies on FRP-confined concrete columns reported in the literature were based on testing of small-scale specimens. In most cases, the specimens tested had a diameter of 150 mm and a height of 305 mm. The experimental investigation of the behaviour of large-scale FRP-confined circular concrete columns has been carried out at the University of Toronto (Jaffry and Sheikh ^[2], and Cairns and Sheikh ^[3]) and is discussed in the following section.

Tests Conducted on Large Scale FRP-Confined Concrete Columns

Twenty-eight nearly full-scale concrete columns were tested under monotonic concentric load at the University of Toronto ^[2,3]. The variables tested in the experimental study included the type of FRP (glass or carbon), the number of layers of FRP, the orientation of fibres in the FRP shell and the amount of lateral reinforcement. All specimens were 356 mm in diameter, standing 1524 mm high. The response of the concrete confined with FRP showed two slopes of the ascending branch before the peak stress. The first slope was approximately equal to that of unconfined concrete. The second slope, being less steep, started near the peak stress of the unconfined concrete and continued until the peak. This was followed by a significant post-peak response that continued until the FRP shell was sufficiently ruptured, resulting in a sudden drop of stress in concrete. Figure 1 shows the axial stress-axial strain curves for some of Toronto specimens, confined with 1 and 2 layers of CFRP and GFRP.

Gradual Rupture of FRP

A careful study of the experimental observations and results ^[1] revealed that the FRP shell does not rupture at once. The failure starts in some fibres at one location due to local crushing/cracking of concrete. Beyond that point the axial stress in concrete stops increasing with the increase in axial strain. As the FRP shell has not ruptured completely, the stress in concrete does not drop rapidly after the peak. Instead, the fibres continue to rupture gradually and the fracture in the shell propagates in both horizontal and vertical directions, until a stage is reached when all the remaining fibres at the fracture locations fail at once, resulting in the ultimate failure of the column. By this time, the concrete inside the FRP shell is already crushed, therefore as soon as the residual FRP fails, the crushed concrete can not take any significant load and the axial stress in concrete drops rapidly. The phenomenon of gradual rupture of FRP is illustrated in Figure 2.

CLASSIFICATION AND COMPARISON OF EXPERIMENTAL DATA

Results from 14 different experimental investigations documented in the published literature ^[1] were compared and analysed. All 77 specimens were confined with carbon or glass FRP. It was observed that the two significant parameters that affect the performance of confined concrete are the confinement pressure f_{con} and the confinement stiffness E_{conf} . The compressive strength of the confined concrete depends on the maximum confining pressure, while the slope of the second ascending branch of stress-strain curve essentially depends on the stiffness of the confining system. The comparative study of the experimental data was therefore divided into two categories based on the confinement pressure and the confinement stiffness. Since there is a wide

range of unconfined concrete compressive strengths of specimens tested in various studies, the analysis was made on the basis of the normalized confinement pressure f_{con}/f'_{co} and the normalized confinement stiffness E_{con}/f'_{co} . Figures 3 and 4 show typical comparison of the normalized stress-strain curves of specimens tested by various researchers, subjected to similar normalized confinement pressure and normalized confinement stiffness, respectively.

A few general observations made from the literature search and comparisons of experimental data are narrated here. Most of the specimens (approximately 81%) tested had section diameter less than or equal to 152 mm. The properties of FRP, lateral confining pressure, stiffness of confinement and specimen size appear to be the main variables that affect concrete behaviour. A comparison of specimens with similar parameters showed a large scatter in the stress-strain behaviour of specimens. Behaviour of confined concrete up to peak stress is almost bilinear for almost all specimens reported. However, only Jaffry and Sheikh ^[2] and Cairns and Sheikh ^[3] reported stable descending branches of FRP-confined concrete response.

Based on the evaluation of existing test data, it was concluded that no analytical model can be expected to predict the behaviour of specimens which behave differently even under similar conditions. To evaluate the existing analytical models or to develop an analytical model to predict the behaviour of FRP-confined concrete columns reasonably accurately, it was essential for the analyses to be performed on specimens that exhibit reliable experimental results. Therefore, twenty specimens (ten tested at the University of Toronto ^[2, 3] and ten tested by other researchers ^[6, 11, 12, 14]) were selected for further analytical investigation. The properties of these specimens are given in Table 1.

PERFORMANCE ANALYSIS OF EXISTING MODELS

A systematic assessment of the performance of six existing analytical models for FRP-confined concrete was conducted ^[1] based on the test data from the twenty selected specimens. The models studied were models proposed by Saadatmanesh, Ehsani and Li ^[4], Samaan, Mirmiran and Shahawy ^[5], Saafi, Toutanji and Li ^[6], Spoelstra and Monti ^[7], Fam and Rizkalla ^[8], and Harries and Kharel ^[9].

Typical stress-strain response predictions from all the six models are shown in Figures 5 and 6 for two of Toronto specimens (confined with two layers of CFRP and GFRP, respectively) and Figures 7 and 8 for two of specimens tested by other researchers. Following brief comments can be made from the comparison of analytical and experimental results for all specimens:

- The model by Harries and Kharel highly underestimates the peak concrete stress. All other models overestimate the peak concrete stress for most specimens. The predictions of the peak concrete stress from the models are comparatively better for specimens tested by other researchers as compared to those for Toronto specimens. Among all the models, the models by Saafi et al. and Samaan et al. give comparatively better predictions for peak stress and strain.
- Although the models, except the one by Saadatmanesh et al., are able to define the bilinear stress-strain response up to the peak stress, they were unable to predict the behaviour of the specimens after the peak concrete stress. This was due to the fact that all these models were based on the assumption that the peak concrete stress is reached at the point when the tensile strain in FRP reaches its ultimate value and the columns fails as soon as the FRP jacket ruptures. However, it has

been observed in experimental results for large-scale specimens ^[2, 3] that the fibres in the FRP jacket fail gradually and once the gradual rupture of FRP jacket starts, the stress-strain curve of concrete enters into the post-peak response.

- Although the model by Saadatmanesh et al. gives the post-peak response for the columns, the predicted post-peak branch is much flatter than those in experimental results. This is again due to the fact the model, being an extension to the model by Mander et al. ^[19] which was proposed for steel-confined concrete columns, generates the whole stress-strain response with a constant value of confining pressure.
- The model by Harries and Kharel also shows a descending branch in stress-strain curves for Toronto specimens. However this descending branch does not represent the post-peak response of the specimen as the stress-strain curve starts descending soon after strain corresponding to unconfined concrete strength is reached and there is no second ascending branch representing confined concrete behaviour. The descending branch for Toronto specimens is due to the fact that the model highly underestimates the confined concrete strength.

It is evident from the analysis that none of the existing models predicts the stress-strain behaviour of the specimens with reasonable accuracy. Therefore the need for a more rational analytical model exists which should be able to accurately predict the complete behaviour of FRP-confined concrete.

THE PROPOSED MODEL

Introduction

Confinement of concrete columns, either by conventional transverse reinforcing steel or external steel/FRP jacket, is a passive phenomenon. In a confined column, at low levels of axial strain in concrete, the transverse reinforcement is hardly stressed and thus the concrete follows the unconfined behaviour. As the axial strain increases, significant micro-cracking occurs in the concrete core and the transverse strains become so high that concrete bears out against the transverse reinforcement, which in turn applies a confining stress to the concrete. That is, the confining pressure on the concrete is developed as an outcome of a restraint to the transverse dilation of the concrete when subjected to axial load.

Most of the traditional confinement models, developed for steel-confined columns, were based on the assumption that steel, being elasto-plastic in nature, applies a uniform confining pressure on the concrete core. This is a reasonable assumption for steel-confined concrete columns, except for the case when the confining steel is still elastic, which occurs at low strains when the response of concrete is still in the ascending portion of its stress-strain curve, or significantly larger amount of confining steel is provided than is needed, such as, in case of concrete filled steel tubes. However, the assumption that concrete is subjected to constant confining pressure is not applicable in case of FRP-confined concrete columns because of a lack of post-peak stress-strain behaviour of FRP. The confining pressure applied on the concrete core by the FRP jacket/shell is linearly increasing until the point where gradual rupture of FRP initiates. After this point the confining pressure keeps decreasing until the residual FRP ruptures.

Description of the confinement model

The incremental procedure originally proposed by Madas and Elnashai ^[10] and later used by Harries and Kharel ^[9] is adopted as the basis for developing the passive confinement model to simulate the response of FRP-confined concrete. A schematic representation of the stress-strain response of the FRP-confined concrete using the new variable confinement model is shown in Figure 9. The loading is considered by imposing an axial strain ε_c . The incremental procedure operates by calculating the lateral strain ε_l corresponding to the current axial strain ε_c , based on the dilation relationship of concrete. The lateral strain is then used to determine the stress in the FRP jacket f_{FRP-i} and the confining pressure f_{con-i} exerted by the FRP jacket. The confined stress-strain relationship for concrete corresponding to that constant confining pressure is thereby calculated and the predicted stress f_c in concrete corresponding to the selected axial strain is determined. This represents one point of the stress-strain plot of concrete subjected to variable confinement. The complete response of concrete is determined by increasing the axial strain and calculating the corresponding axial stress based on the confining pressure obtained in each increment. Therefore, the final response of the confined concrete crosses a series of hypothetical curves representing the responses of concrete under different levels of constant confining pressures. To use this incremental procedure, following four relationships need to be defined:

I. Stress-strain relationship of concrete under constant confining pressure:

Following equation originally proposed by Popovics ^[18] for unconfined concrete and later used by Mander et al. ^[19] is adopted:

$$f_c = \frac{f'_{ccmax} x r}{r - 1 + x'} \quad (1)$$

$$\text{where } x = \frac{\varepsilon_c}{\varepsilon'_{ccmax}}, \quad r = \frac{E_c}{E_c - E_{sec}}, \quad E_{sec} = \frac{f'_{ccmax}}{\varepsilon'_{ccmax}} \quad (2)$$

where E_c is the tangent modulus of elasticity of concrete, E_{sec} is the secant modulus of elasticity of confined concrete at peak stress, f_c and ε_c are current axial stress and axial strain in concrete, respectively, f'_{ccmax} is the compressive strength of confined concrete subject to constant confining pressure. It should be noted that f'_{ccmax} is not the actual compressive strength f'_{cc} of the passively confined concrete. Instead, it is the peak stress of the hypothetical stress-strain curve defined for a particular confining pressure to obtain the stress in concrete corresponding to the imposed axial strain. The actual compressive strength f'_{cc} of the passively confined concrete will be known after generating the complete stress-strain response of the confined concrete. Following equation is proposed to determine f'_{ccmax} :

$$f'_{ccmax} = f'_{co} + 6.4 \left(f'_{con-i} \right)^{0.9} \quad (3)$$

ε'_{ccmax} is the strain corresponding to f'_{ccmax} , for which the following equation proposed by Mander et al. ^[19] is adopted:

$$\varepsilon'_{ccmax} = \varepsilon'_{co} \left(5 \frac{f'_{ccmax}}{f'_{co}} - 4 \right) \quad (4)$$

where, f'_{co} and ε'_{co} are the compressive strength and corresponding axial strain of unconfined concrete, respectively, and f'_{con-i} is the confining pressure applied by the FRP jacket at a particular strain increment.

II. The dilation ratio ν of concrete:

The dilation ratio or the secant Poisson's ratio is the ratio of lateral strain to axial strain in concrete at any given strain increment. For determining the confining pressure acting on the concrete core and thus the stress-strain response of confined concrete, the dilation response of concrete must be clearly understood.

The experimental axial stress-lateral strain and lateral strain-axial strain responses of specimens confined with 1- and 2-layers of GFRP (specimens G01-00-9 and G01-00-11) tested by Jaffry and Sheikh ^[2] are shown in Figures 10 and 11, respectively. It can be observed in Figure 11 that during the initial stages of loading (at low axial strain levels), the dilation ratio ν of concrete remains constant and close to the initial Poisson's ratio ν_o of unconfined concrete. During this phase, concrete behaves elastically and follows unconfined behaviour (Figure 10). As the axial strain increases, the concrete starts dilating with a higher rate and the dilation ratio continues to increase until the stage is reached where the confining FRP jacket has become fully activated. At this point, the dilation ratio stops increasing and remains constant until the peak load. This final constant value is termed the maximum dilation ratio ν_{max} . Similar observations regarding the dilation behaviour of concrete have been reported by previous researchers ^[5, 8, 9, 11, 12, 13]. It was also reported that the maximum dilation ratio depends on the stiffness of the confining system and the compressive strength of concrete. Maximum dilation ratio is higher for lower confinement stiffness and higher concrete strength. This fact can also be observed in Figure 11. The maximum dilation ratio is reported as low as 0.20 ^[11, 13].

Based on the observations made here and those reported by previous researchers, following relationship is used to determine the dilation ratio of concrete corresponding to the current axial strain ϵ_c :

$$\text{For } \varepsilon_c \leq 0.60\varepsilon'_{co} \quad \nu = \nu_o \quad (5)$$

$$\text{For } \varepsilon_c > 0.60\varepsilon'_{co} \quad \nu = \nu_o \left[1 + 1.5 \left(2 \frac{\varepsilon_c}{\varepsilon'_{co}} - 1 \right)^2 \right] \leq \nu_{\max}$$

Equation (5) proposed by Vecchio ^[20] for steel reinforced concrete had a maximum limit of $\nu_{\max} = 0.50$. For concrete confined with FRP, Equation (6) is proposed. Based on the experimental results reported in the literature, a lower limit of 0.20 is suggested for ν_{\max} .

$$\nu_{\max} = -0.418 \left(\frac{E_{conf}}{f'_{co}} \right) + 1.851 = -0.418 \left(\frac{2nE_{FRP}}{Df'_{co}} \right) + 1.851 \quad (6)$$

where E_{FRP} is the modulus of elasticity of FRP in the units of force/width, n is the number of layers of FRP and D is the diameter of column.

The current concrete lateral strain ε_l which is also the tensile strain in the FRP shell for the case of circular cross-section, is calculated from sectional equilibrium as:

$$\varepsilon_l = \nu \varepsilon_c \quad (7)$$

III. Stress-strain relationship of FRP:

The FRP jacket is assumed to exhibit linear-elastic stress-strain response until failure. Since the thickness of the FRP shell is usually not uniform due to the manual lay-up of FRP, the tensile strength f_{FRPu} and modulus of elasticity E_{FRP} of the FRP shell are expressed in the units of force per unit width instead of force per unit area. Therefore, phenomenon of gradual rupture of FRP is accounted for by reducing the number of layers of FRP. Thus, a new value of number of layers of FRP n_i is calculated in each increment by the following equation:

$$n_i = n \left[1 - (1-r) \left(\frac{\varepsilon_l - f \varepsilon_{FRPu}}{\varepsilon_{FRPu} - f \varepsilon_{FRPu}} \right) \right] \quad (8)$$

where ε_{FRPu} is the rupture strain of FRP as obtained from tensile coupon tests, f is the ratio of stress in the FRP shell at which gradual rupture starts to the tensile strength of FRP, and r is the fraction of the original FRP fibres that remains at the ultimate point when the stress in the residual fibres reaches the ultimate. Based on a parametric study^[1] conducted during this research, it is suggested to use a value of 0.5 for both f and r .

The tensile force/width f_{FRP-i} in the FRP corresponding to the current axial strain is calculated as follows:

$$f_{FRP-i} = E_{FRP} \varepsilon_l \quad (9)$$

IV. Relationship between stress in FRP jacket and confining pressure:

Considering the equilibrium of the circular cross-section and assuming that the confining pressure f_{con-i} is distributed uniformly over the concrete surface, the confining pressure at any axial strain increment is calculated by:

$$f_{con-i} = \frac{2n_i f_{FRP-i}}{D} = \frac{2n_i E_{FRP} \varepsilon_l}{D} \quad (f_{FRP.i} \text{ and } E_{FRP} \text{ in force/width}) \quad (10)$$

APPLICATION OF PROPOSED CONFINEMENT MODEL

The proposed model was applied to the selected twenty specimens (Table 1). The typical comparisons of analytical and experimental stress-strain responses are shown in Figures 12 and 13 for two of specimens tested at the University of Toronto and in Figures 14 and 15 for two specimens tested by other researchers, respectively. From the results of all the specimens, following brief comments are made:

- The proposed model is able to predict the complete stress-strain response of selected specimens with reasonable accuracy. The predicted stress-strain curves have a good agreement with experimental curves in terms of slopes of first and second ascending branches, confined concrete strength, the corresponding axial strain, and shape and slope of post-peak branch.
- The overall average ratio of analytical to experimental confined concrete strength for all the specimens is 1.00. The corresponding axial strain ratio is 0.99. The predictions for confined concrete strength are better than those for the corresponding axial strain.
- As compared to previous models, the proposed model predicted the results with much better accuracy. The comparison of analytical and experimental values of confined concrete strength and corresponding axial strain from all the 7 models are shown in Figures 16 and 17, respectively, for Toronto specimens and in Figures 18 and 19, respectively, for other specimens. The ratio of analytical to experimental concrete strength from previous models ranges between 0.59 and 1.43 for Toronto specimens and between 0.60 and 1.24 for other specimens, whereas this ratio from the proposed model ranges between 0.91 and 1.07 for Toronto specimens and between 0.92 and 1.03 for other specimens. The ratio of analytical to experimental axial strain corresponding to peak stress from previous models ranges between 0.19 and 3.60 for Toronto specimens and between 0.44 and 1.96 for other specimens, whereas this ratio from the proposed model varies between 0.83 and 1.35 for Toronto specimens and between 0.51 and 1.14 for other specimens.

It is concluded that the proposed model predicts the response of selected specimens with reasonable accuracy. Analytical results from the proposed model are marked improvements over the existing models.

CONCLUSIONS

There exists a considerable scatter in the experimental stress-strain behaviour of specimens tested by various researchers subjected to similar confinement levels. Moreover, the specimens tested by several researchers did not have a post-peak response reported. However, the large-scale specimens tested at the University of Toronto exhibited considerable post-peak response before the complete failure.

The existing analytical models for FRP-confined concrete failed to accurately predict the complete stress-strain response of specimens reported in the literature. Particularly, the models were unable to simulate the post-peak response. An analytical model has been proposed that takes into account the progressive failure of FRP confining reinforcement and displays post-peak response of confined concrete. The predictions of the proposed model for confined concrete strength, corresponding axial strain and entire stress-strain response of selected specimens were found to be reasonably accurate and a significant improvement over the previous models.

ACKNOWLEDGEMENTS

The research reported was supported by grants from Natural Sciences and Engineering Research Council (NSERC) of Canada and ISIS Canada, an NSERC

network of Centers of Excellence. Additional financial support from Fyfe and Co., R. J. Watson, Inc. and Kinetics, Inc. is gratefully acknowledged.

REFERENCES

1. Samdani, S., “Analytical Study of FRP-Confined Concrete Columns”, M.A.Sc. Thesis, Dept. of Civil Engineering, University of Toronto, Toronto, Canada, 2003.
2. Jaffry, S.A.D. and Sheikh, S.A., “Concrete Filled Glass Fiber Reinforced Polymer (GFRP) Shells under Concentric Compression”, Dept. of Civil Engineering, University of Toronto, Research Report: SJ-01-01, April 2001.
3. Cairns, S.W. and Sheikh, S.A., “Circular Concrete Columns Externally Reinforced with Pre-Fabricated Carbon Polymer Shells”, Dept. of Civil Engineering, University of Toronto, Research Report: CS-01-01, October 2001.
4. Saadatmanesh, H. and Ehsani, M.R., “Strength and Ductility of Concrete Columns Externally Reinforced with Fibre Composite Straps”, ACI Structural Journal, V. 91, No. 4, July-August 1994, pp. 434-447.
5. Samaan, M., Mirmiran, A. and Shahawy, M., “Model of Confined Concrete by Fiber Composites”, Journal of Structural Engineering, ASCE, V. 124, No. 9, September 1998, pp. 1025-1031.
6. Saafi, M., Toutanji, A.H. and Li, Z., “Behaviour of Concrete Columns Confined with Fibre Reinforced Polymer Tubes”, ACI Materials Journal, V. 96, No. 4, July-August 1999, pp. 500-509.
7. Spoelstra, M.R. and Monti, G., “FRP-Confined Concrete Model”, Journal of Composites for Construction, ASCE, V. 3, No. 3, August 1999, pp. 143-150.

8. Fam, A.Z. and Rizkalla, S.H., “Confinement Model for Axially Loaded Concrete Confined by Circular Fibre-Reinforced Polymer Tubes”, *ACI Structural Journal*, V. 98, No. 4, July-August 2001, pp. 451-461.
9. Harries, K.A. and Kharel, G., “Behaviour and Modelling of Concrete Subject to Variable Confining Pressure”, *ACI Materials Journal*, V. 99, No. 2, March-April 2002, pp. 180-189.
10. Madas, P. and Elnashai, A.S., “A New Passive Confinement Model for the Analysis of Concrete Structures Subjected to Cyclic and Transient Dynamic Loading”, *Earthquake Engineering and Structural Dynamics*, V. 21, 1992, pp. 409-431.
11. Xiao, Y. and Wu, H., “Compressive Behaviour of Concrete Confined by Carbon Fiber Composite Jackets”, *Journal of Materials in Civil Engineering*, ASCE, V. 12, No. 2, May 2000, pp. 139-146.
12. Mirmiran, A.; and Shahawy, M., “Behaviour of Concrete Columns Confined by Fiber Composites”, *Journal of Structural Engineering*, ASCE, Vol. 123, No. 5, May 1997, pp. 583-590.
13. Shahwy, M.; Mirmiran, A.; and Bietelman, T., “Tests and Modeling of Carbon-Wrapped Concrete Columns”, *Composites Part B: Engineering*, Vol. 31, No. 6, Elsevier Science Ltd, London, UK, 2000, pp. 471-480.
14. Matthys, S.; Taerwe, L; and Audenaert, K., “Tests on Axially Loaded Concrete Columns Confined by Fibre Reinforced Polymer Sheet Wrapping”, *4th International Symposium on Fibre Reinforced Polymer Reinforcement for Reinforced Concrete Structures*, 1999, pp. 230-243.

15. Purba, B. K.; and Mufti, A. A., “Investigation of the Behaviour of Circular Concrete Columns Reinforced with Carbon Fibre Reinforced Polymer (CFRP) Jackets”, Canadian Journal of Civil Engineering, Vol. 26, No. 5, October 1999, pp. 590-596.
16. Demers, M.; and Neale, K. W., “Confinement of Reinforced Concrete Columns with Fibre-Reinforced Composite Sheets – An Experimental Study”, Canadian Journal of Civil Engineering, Vol. 26, No. 2, April 1999, pp. 226-241.
17. Nanni, A.; and Bradford, N. M., “FRP Jacketed Concrete under Uniaxial Compression”, Construction and Building Materials, V. 9, No. 2, 1995, pp. 115-124.
18. Popovics, S., “A Numerical Approach to the Complete Stress-Strain Curves for Concrete”, Cement and Concrete Research, V. 3, No. 5, 1973, pp. 583-599.
19. Mander, J.B., Priestly, M.J.N. and Park, R., “Theoretical Stress-Strain Model for Confined Concrete”, Journal of Structural Engineering, ASCE, V. 114, No. 8, August 1988, pp. 1804-1826.
20. Vecchio, F.J., “Finite Element Modelling of Concrete Expansion and Confinement”, Journal of Structural Engineering, ASCE, V. 118, No. 9, September 1992, pp. 2390-2406.

NOTATIONS

ε_c = current axial strain in concrete

ε'_{co} = axial strain corresponding to unconfined concrete strength f'_{co}

ε'_{cc} = axial strain corresponding to confined concrete strength f'_{cc}

ε'_{ccmax} = axial strain corresponding to compressive strength of confined concrete subject to constant confining pressure f'_{ccmax}

ε_{FRPu} = rupture strain of FRP

ε_l = lateral strain in concrete = tensile strain in FRP

ν = current dilation ratio of concrete

ν_o = initial Poisson's ratio of unconfined concrete

ν_{max} = maximum dilation ratio of confined concrete

D = diameter of column

E_c = tangent modulus of elasticity of concrete

E_{conf} = confinement stiffness of confining FRP

E_{FRP} = modulus of elasticity of FRP in the units of force/width

E_{sec} = secant modulus of elasticity of confined concrete at peak stress f'_{cc}

f = ratio of stress in the FRP shell at which gradual rupture starts to FRP tensile strength

f_c = current axial stress in concrete

f'_{co} = compressive strength of unconfined concrete

f'_{cc} = compressive strength of confined concrete

f'_{ccmax} = compressive strength of confined concrete subject to constant confining pressure

f_{con} = maximum confinement pressure that FRP can apply

f_{con-i} = current confining pressure applied by FRP at a particular strain increment

f_{FRP-i} = current tensile stress in the FRP in the units of force/width

f_{FRPu} = tensile strength of FRP in the units of force/width

n = total number of layers of FRP

n_i = current number of layers of FRP at a particular strain increment

r = fraction of the original FRP fibres that remains at the ultimate point when the stress in the residual fibres reaches the ultimate.

LIST OF TABLES

Table 1: Properties of specimens selected for the analyses

LIST OF FIGURES

Figure 1: Experimental stress-strain curves for Toronto specimens ^[2, 3]

Figure 2: Gradual rupture of FRP

Figure 3: Experimental stress-strain curves for specimens with similar f_{con}

Figure 4: Experimental stress-strain curves for specimens with similar E_{con}

Figure 5: Stress-strain response prediction of existing models for Specimen C02-00-24

Figure 6: Stress-strain response prediction of existing models for Specimen G02-00-11

Figure 7: Stress-strain response prediction of existing models for Specimen STL-C2

Figure 8: Stress-strain response prediction of existing models for Specimen XW-2

Figure 9: Schematic representation of proposed confinement model

Figure 10: Experimental axial stress-lateral strain response for two of Toronto specimens

Figure 11: Experimental lateral strain-axial strain response for two of Toronto specimens

Figure 12: Stress-strain response prediction of proposed model for Specimen C02-00-24

Figure 13: Stress-strain response prediction of proposed model for Specimen G02-00-11

Figure 14: Stress-strain response prediction of proposed model for Specimen STL-C2

Figure 15: Stress-strain response prediction of proposed model for Specimen XW-2

Figure 16: Comparison of all models for prediction of f'_{cc} for Toronto Specimens

Figure 17: Comparison of all models for prediction of ε'_{cc} for Toronto Specimens

Figure 18: Comparison of all models for prediction of f'_{cc} for Other Specimens

Figure 19: Comparison of all models for prediction of ε'_{cc} for Other Specimens

Table 1: Properties of specimens selected for the analyses

S.No.	Specimen Classification		Geometry		Concrete Properties			FRP Properties			Confinement Properties			Experimental Results					
	Researcher	Specimen designation	FRP type	D (mm)	L (mm)	f'_{co} (MPa)	ϵ'_{co} (mm/m)	E_c (MPa)	n	f_{FRP} (N/mm)	ϵ_{FRP} (mm/m)	E_{FRP} (N/mm)	E_{conf} (MPa)	f_{con} (MPa)	E_{conf}/f_{co}	f_{co} (MPa)	ϵ'_{co} (mm/m)	f'_{co}/ϵ'_{co}	
TORONTO SPECIMENS																			
1		C01-L0-20		356.0	1524	32.2	1.80	29300	1	885.0	21.5	41163	231	4.97	7.17	0.154	43.9	8.88	4.93
2	Cairns &	C01-LS320-21		356.0	1524	31.4	1.80	29300	1	885.0	21.5	41163	231	4.97	7.37	0.159	43.4	9.44	5.24
3	Sheikh [3]	C02-00-24	Carbon	356.0	1524	32.4	1.80	29300	2	885.0	21.5	41163	463	9.94	14.26	0.307	59.3	13.75	7.64
4		C02-L0-26		356.0	1524	32.6	1.80	29300	2	885.0	21.5	41163	463	9.94	14.17	0.305	59.3	17.89	9.94
5		C02-LS320-27		356.0	1524	32.6	1.80	29300	2	885.0	21.5	41163	463	9.94	14.17	0.305	57.0	14.42	8.01
6		G01-00-7		356.0	1524	29.2	1.80	29300	1	535.0	23.7	22574	127	3.01	4.34	0.103	34.8	3.70	2.06
7	Jaffry &	G01-L0-9		356.0	1524	29.2	1.80	29300	1	535.0	23.7	22574	127	3.01	4.34	0.103	32.4	7.39	4.11
8	Sheikh [2]	G01-LS320-10	Glass	356.0	1524	29.2	1.80	29300	1	535.0	23.7	22574	127	3.01	4.34	0.103	37.2	11.51	6.39
9		G02-00-11		356.0	1524	29.2	1.80	29300	2	535.0	23.7	22574	254	6.01	8.69	0.206	44.8	11.99	6.66
10		G02-LS320-14		356.0	1524	29.2	1.80	29300	2	535.0	23.7	22574	254	6.01	8.69	0.206	49.3	17.92	9.96
11	Matthys et al.	MTA-C240b		150.0	300	34.9	2.10	N/A	1	304.2	11.8	25780	344	4.06	9.85	0.116	46.1	9.00	4.29
12	[14]	MTA-C640b		150.0	300	34.9	2.10	N/A	1	258.5	2.2	117500	1567	3.45	44.89	0.099	45.8	6.00	2.86
13	Xiao & Wu [11]	XW-2	Carbon	152.0	305	33.7	N/A	N/A	2	600.8	15.0	40056	1054	15.81	31.28	0.469	75.5	22.06	N/A
14		STL-C1		152.4	435	35.0	2.50	30000	1	363.0	9.0	40370	530	4.76	15.14	0.136	55.0	10.00	4.00
15		STL-C2		152.4	435	35.0	2.50	30000	2	408.3	9.1	44850	1177	10.72	33.63	0.306	68.0	16.00	6.40
16	Seafi et al. [6]	STL-GE1		152.4	435	35.0	2.50	30000	1	360.0	14.1	25600	336	4.72	9.60	0.135	52.8	19.00	7.60
17		STL-GE2		152.4	435	35.0	2.50	30000	2	404.0	14.9	27200	714	10.60	20.40	0.303	66.0	24.70	9.88
18		STL-GE3	Glass	152.4	435	35.0	2.50	30000	3	448.0	15.6	28800	1134	17.64	32.40	0.504	83.0	30.00	12.00
19	Mirriran &	MS-C1		152.5	305	32.0	N/A	N/A	6	125.8	14.1	8936	703	9.90	21.99	0.310	60.8	34.30	N/A
20	Shahawy [12]	MS-C2		152.5	305	32.0	N/A	N/A	10	127.4	14.4	8874	1164	16.71	36.40	0.523	77.4	37.90	2.42

N/A = Not available in the published reference document

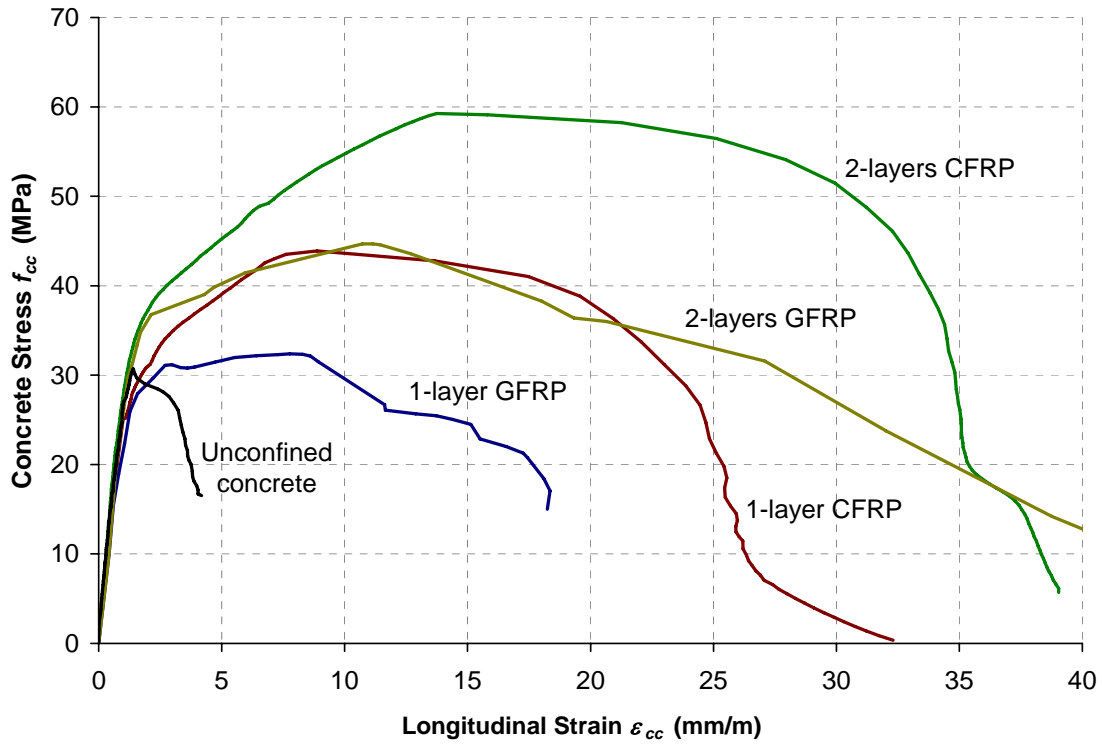


Figure 1: Experimental stress-strain curves for Toronto specimens ^[2, 3]

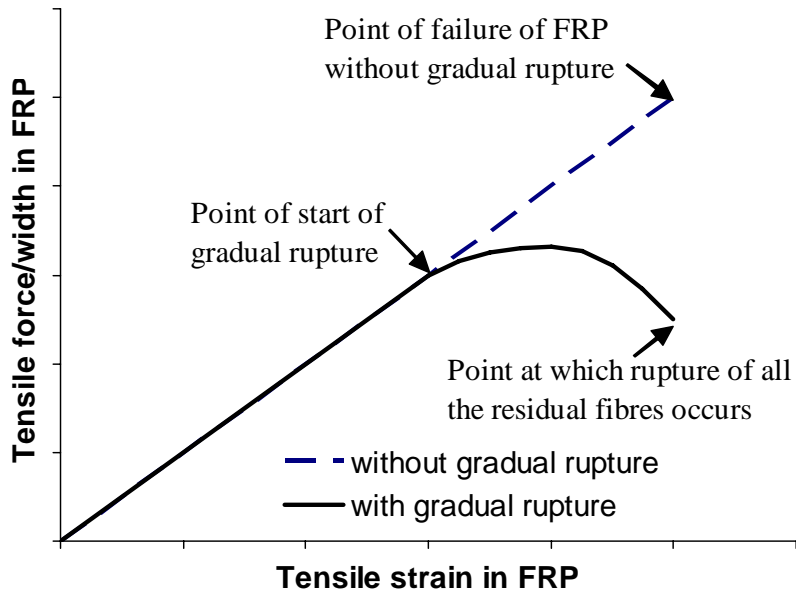


Figure 2: Gradual rupture of FRP

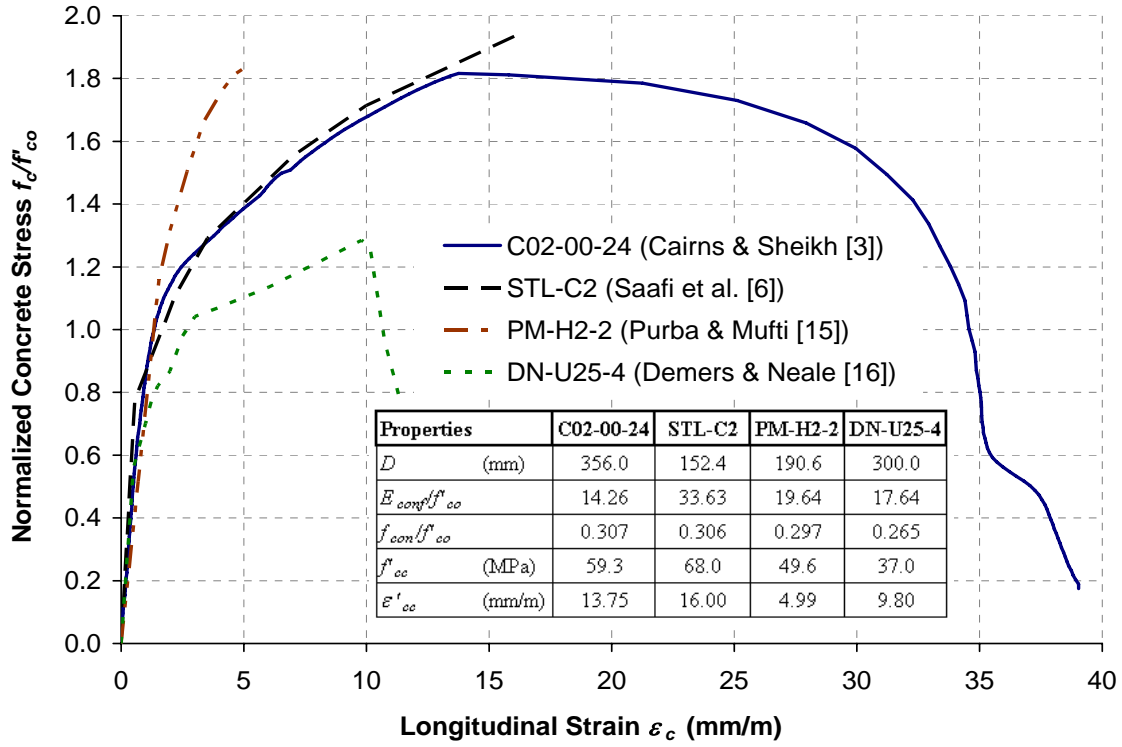


Figure 3: Experimental stress-strain curves for specimens with similar f_{con}

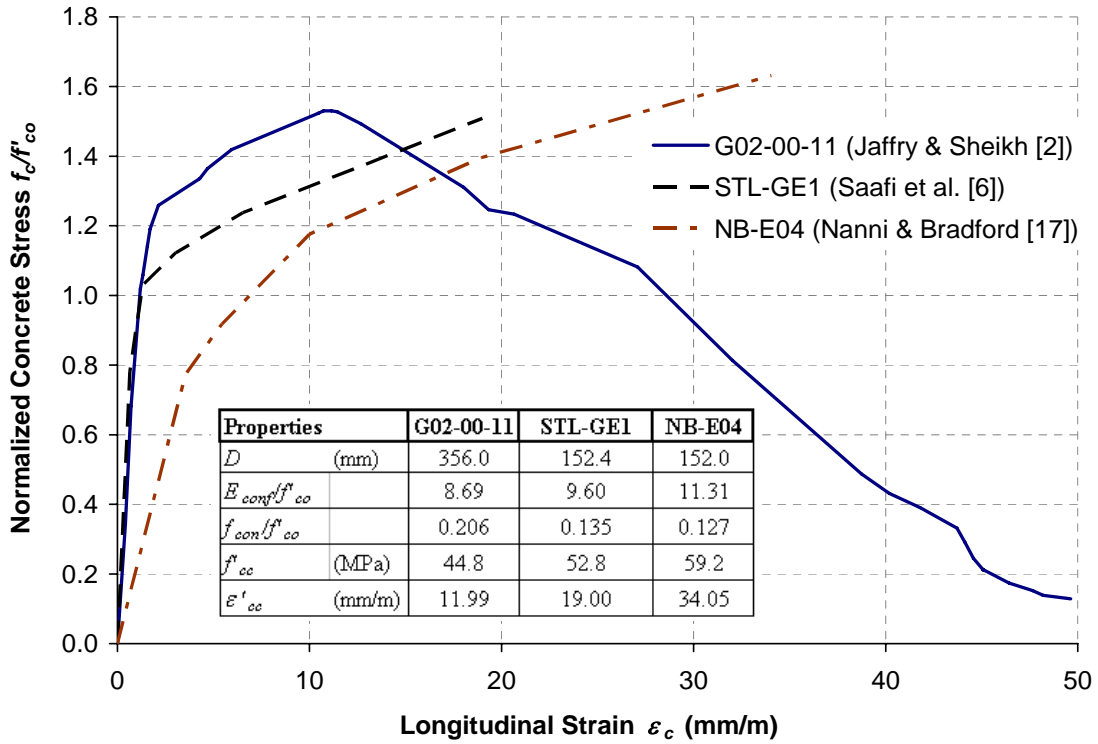


Figure 4: Experimental stress-strain curves for specimens with similar E_{con}

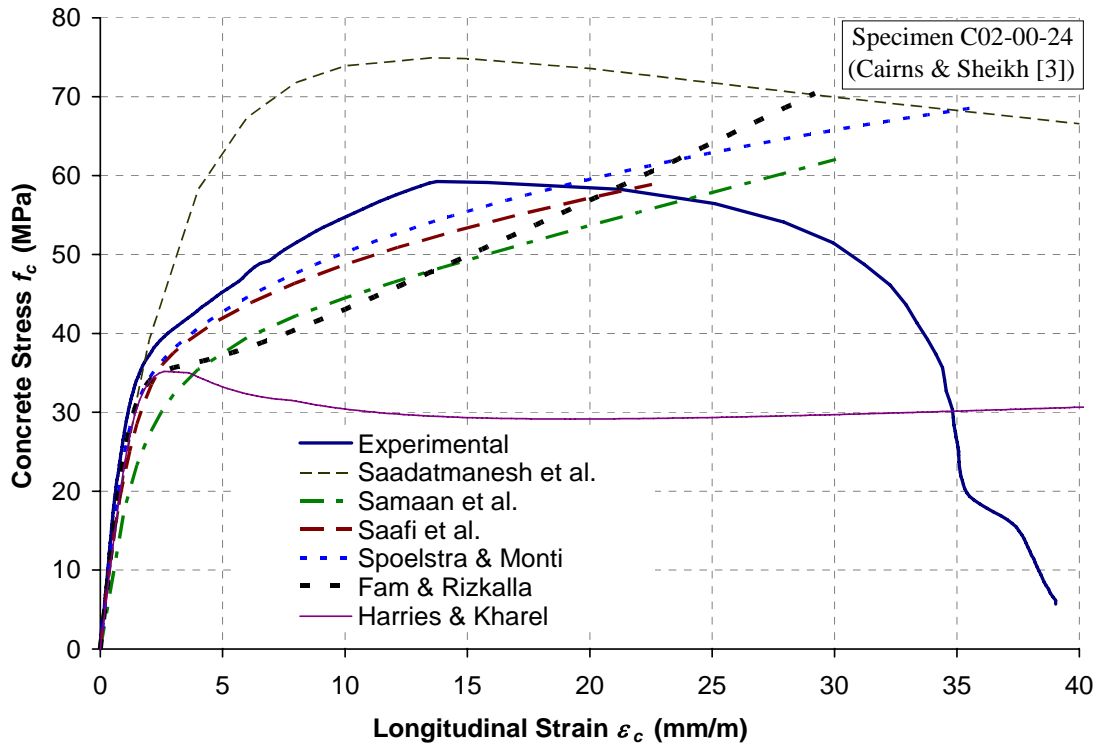


Figure 5: Stress-strain response prediction of existing models for Specimen C02-00-24

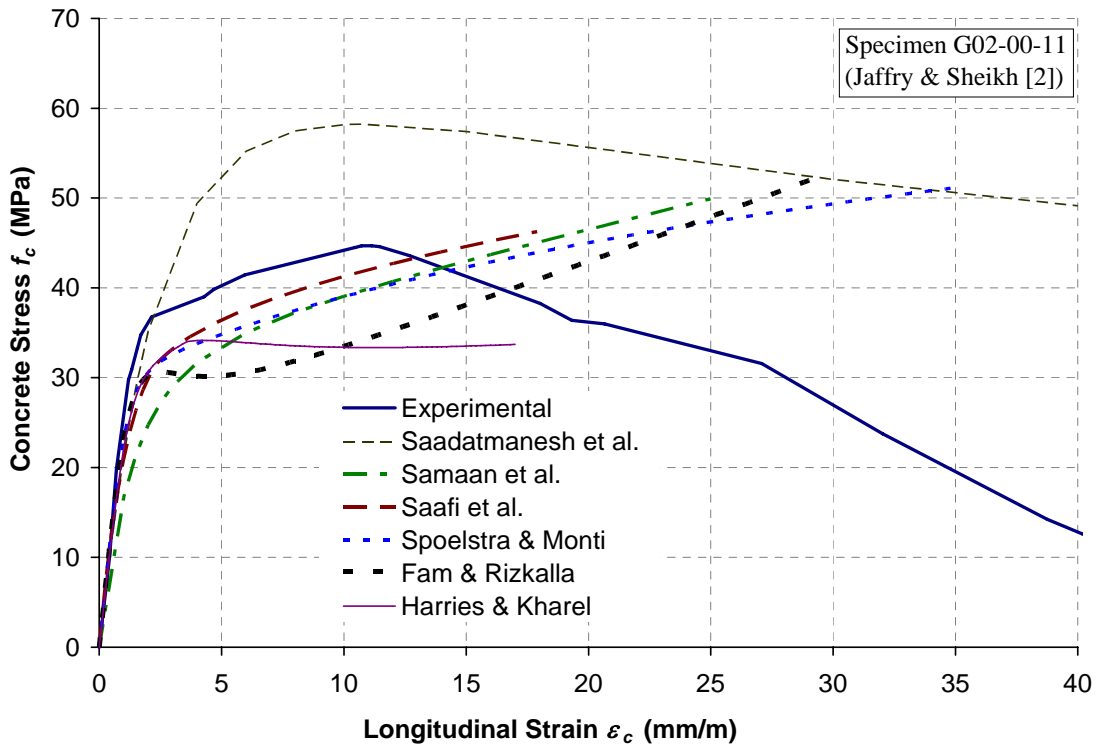


Figure 6: Stress-strain response prediction of existing models for Specimen G02-00-11

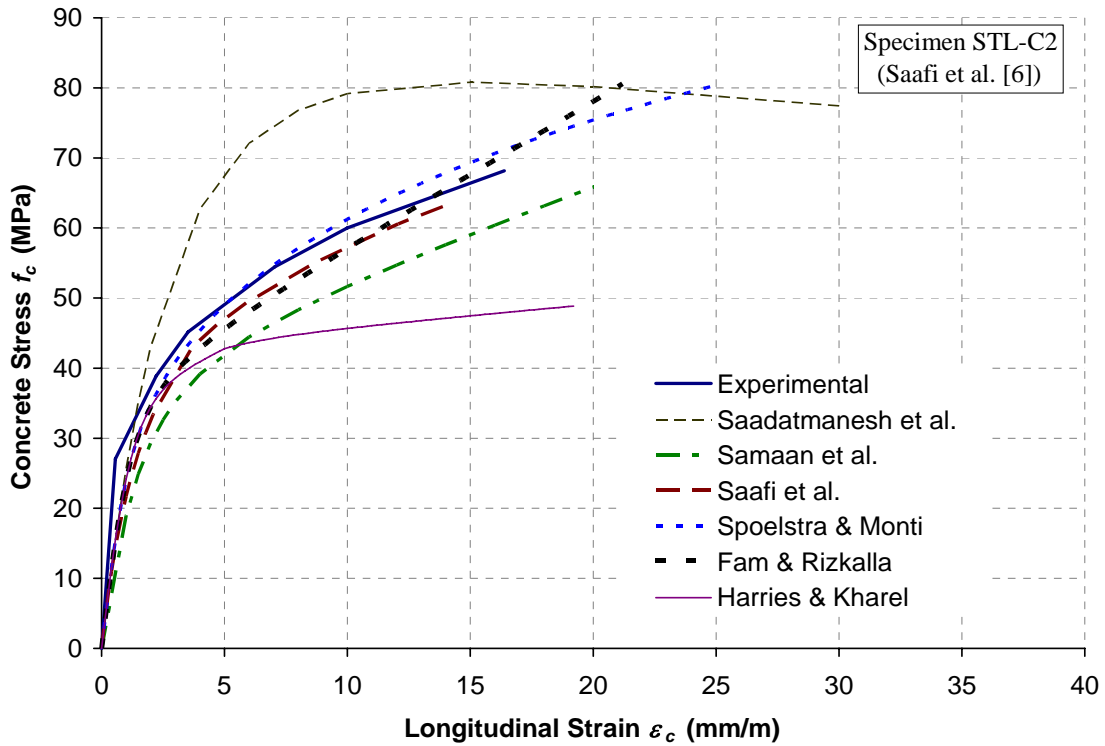


Figure 7: Stress-strain response prediction of existing models for Specimen STL-C2

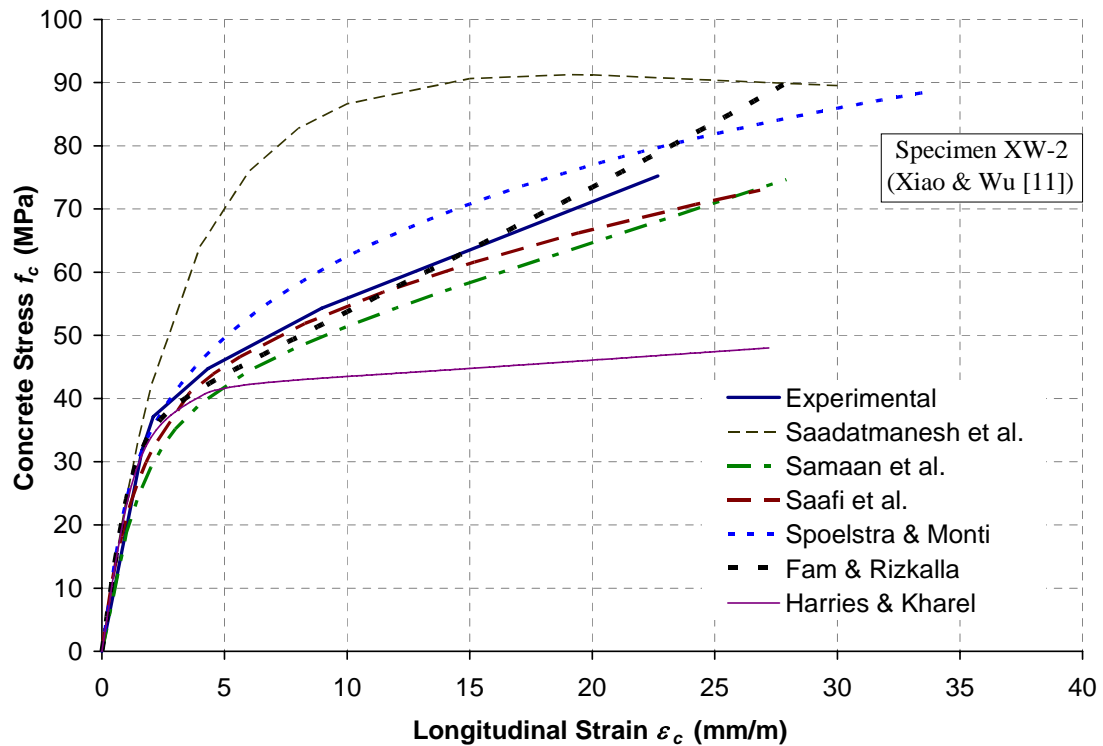


Figure 8: Stress-strain response prediction of existing models for Specimen XW-2

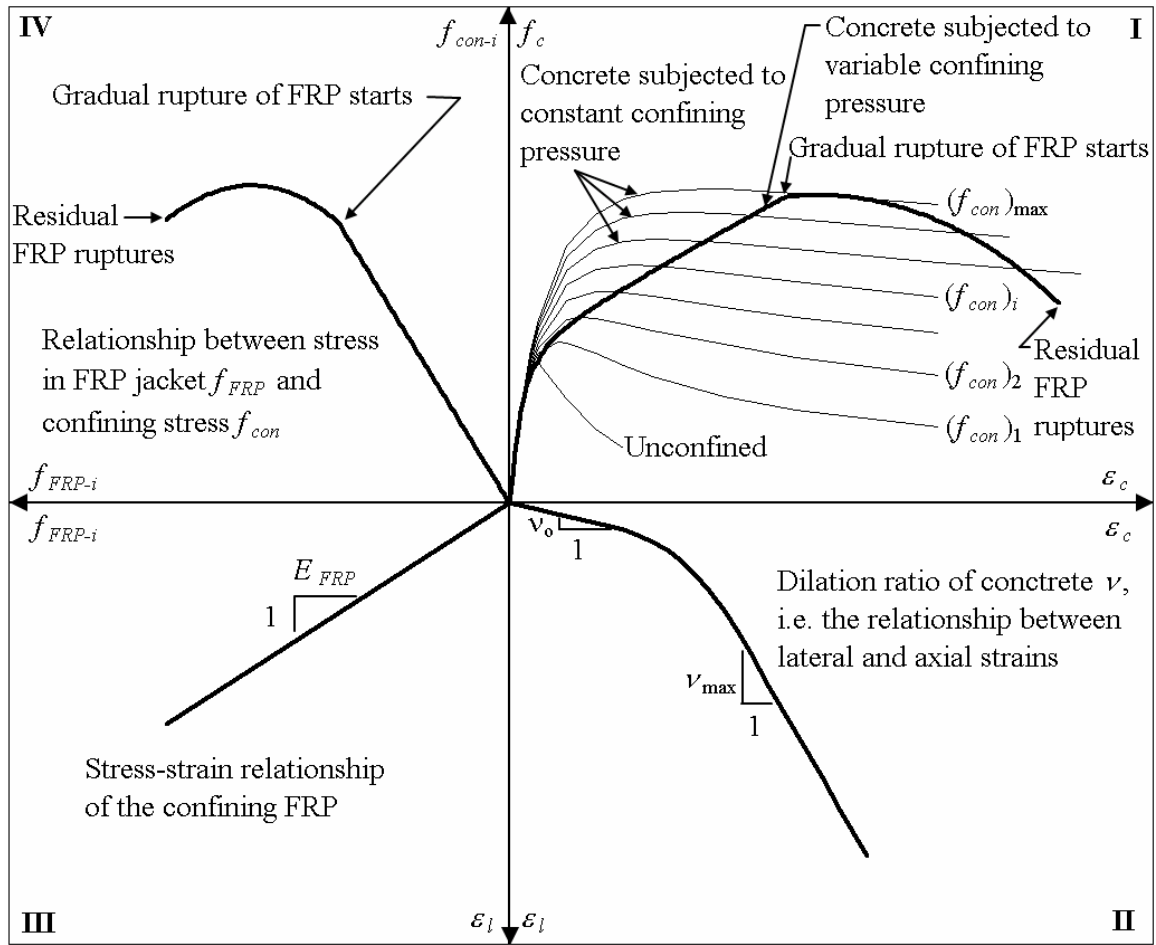


Figure 9: Schematic representation of proposed confinement model

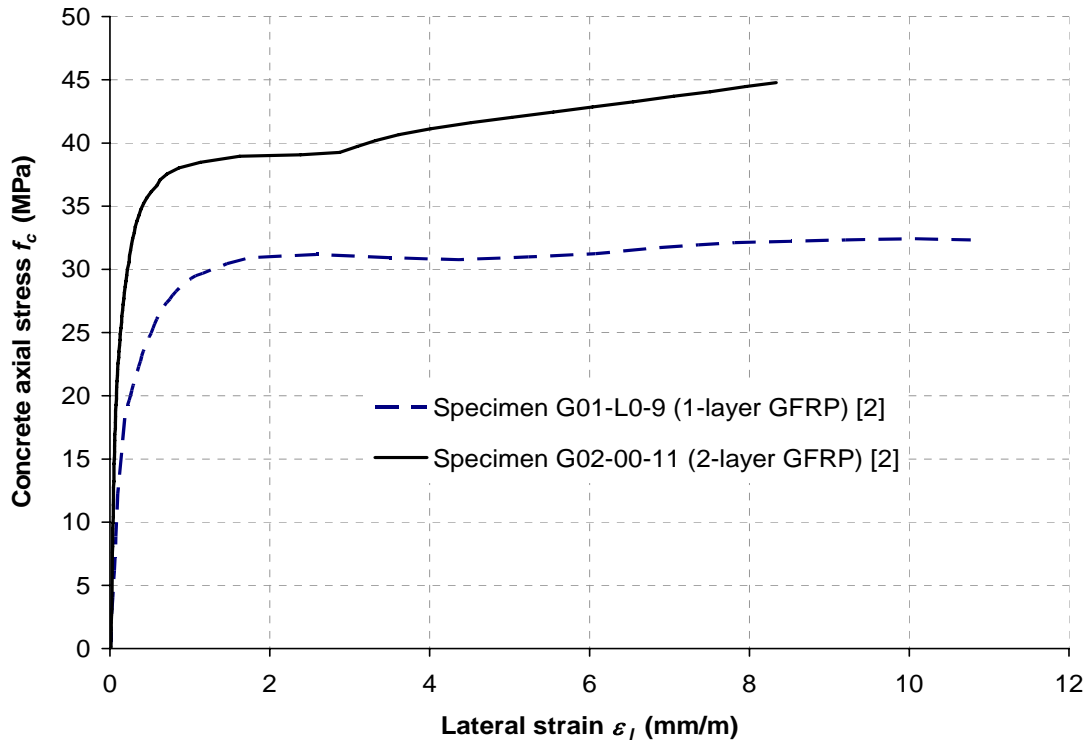


Figure 10: Experimental axial stress-lateral strain response for two of Toronto specimens

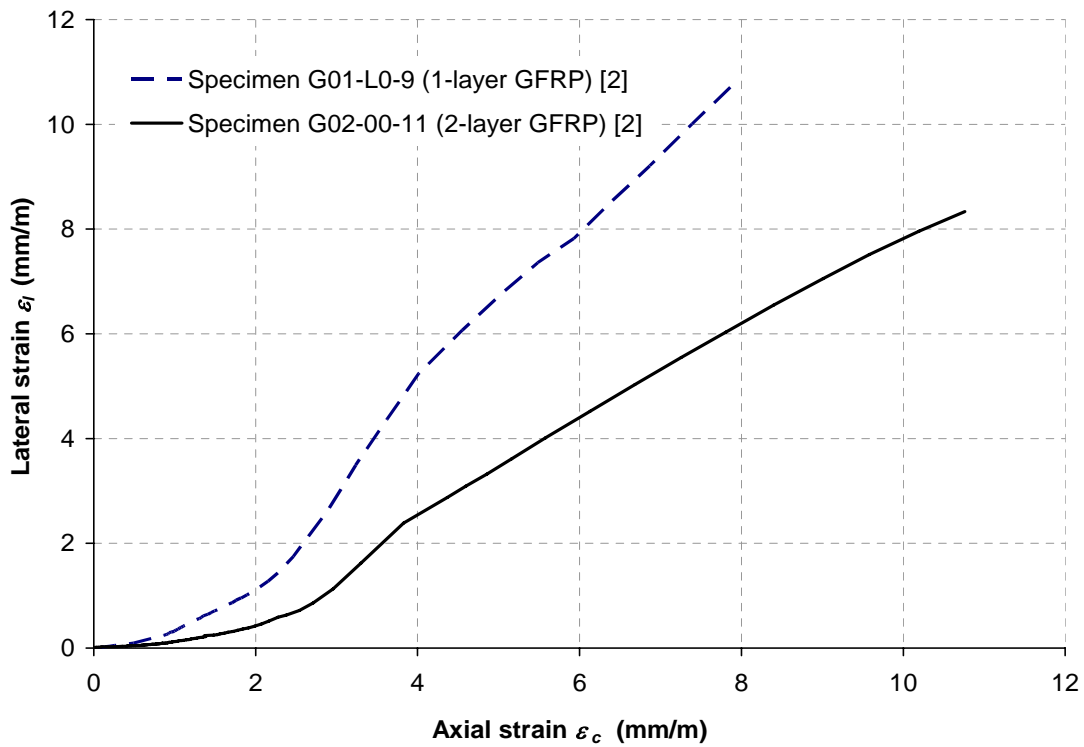


Figure 11: Experimental lateral strain-axial strain response for two of Toronto specimens

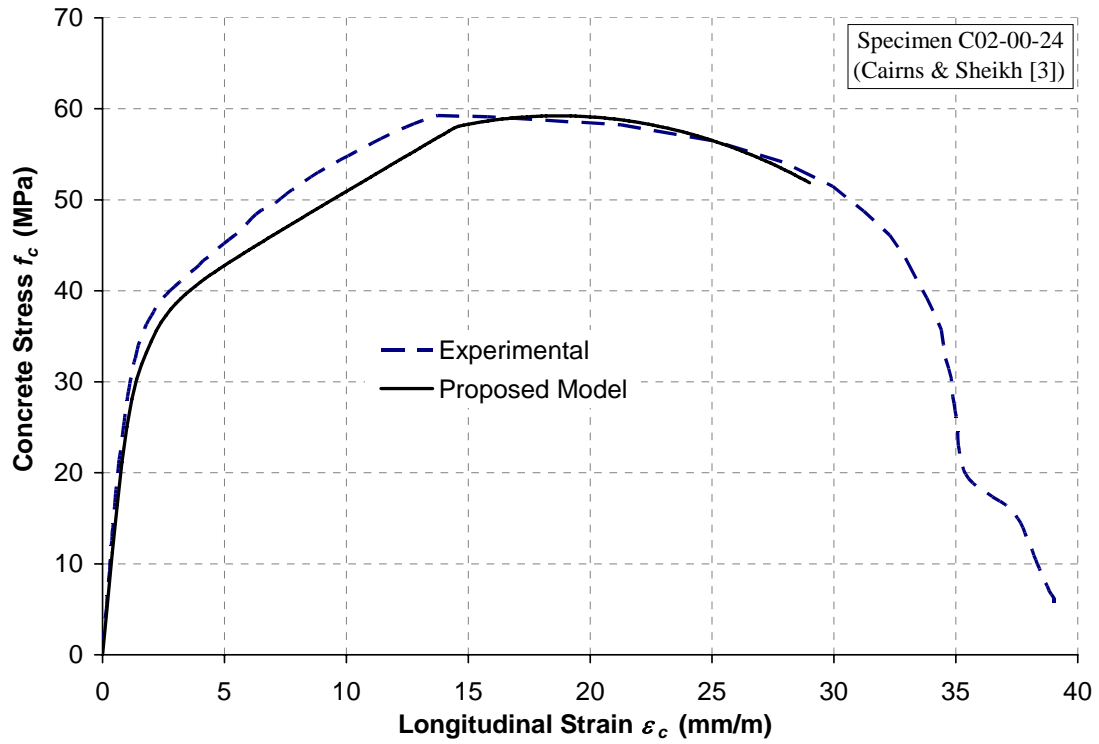


Figure 12: Stress-strain response prediction of proposed model for Specimen C02-00-24

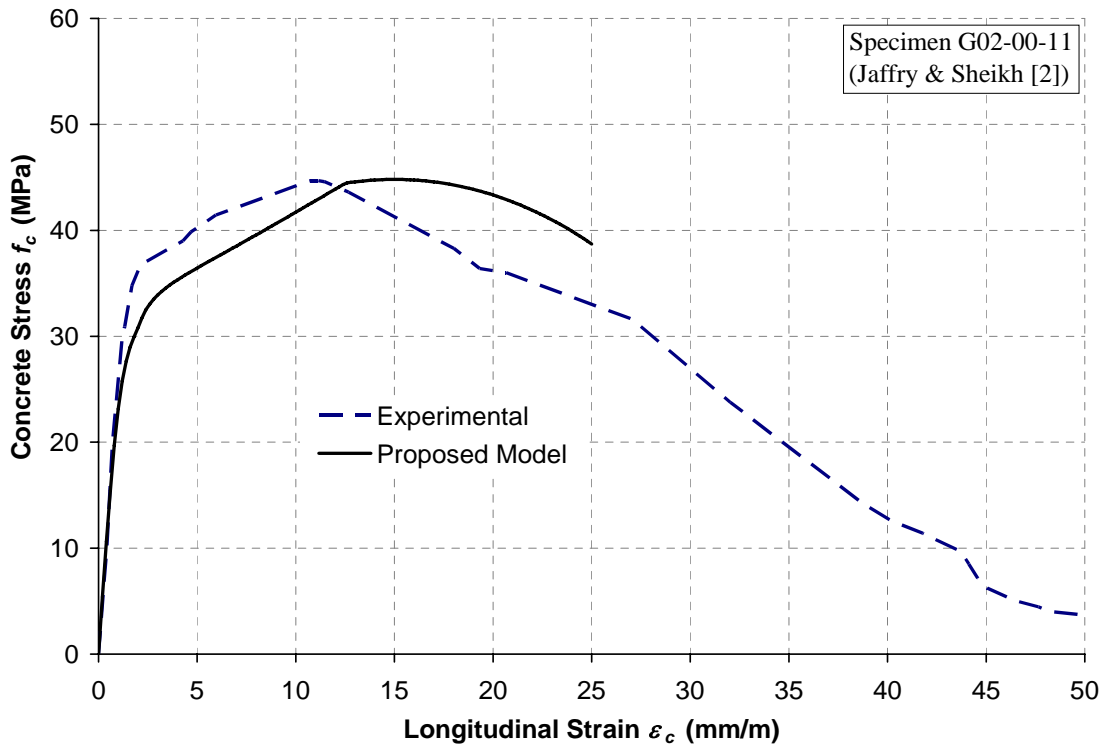


Figure 13: Stress-strain response prediction of proposed model for Specimen G02-00-11

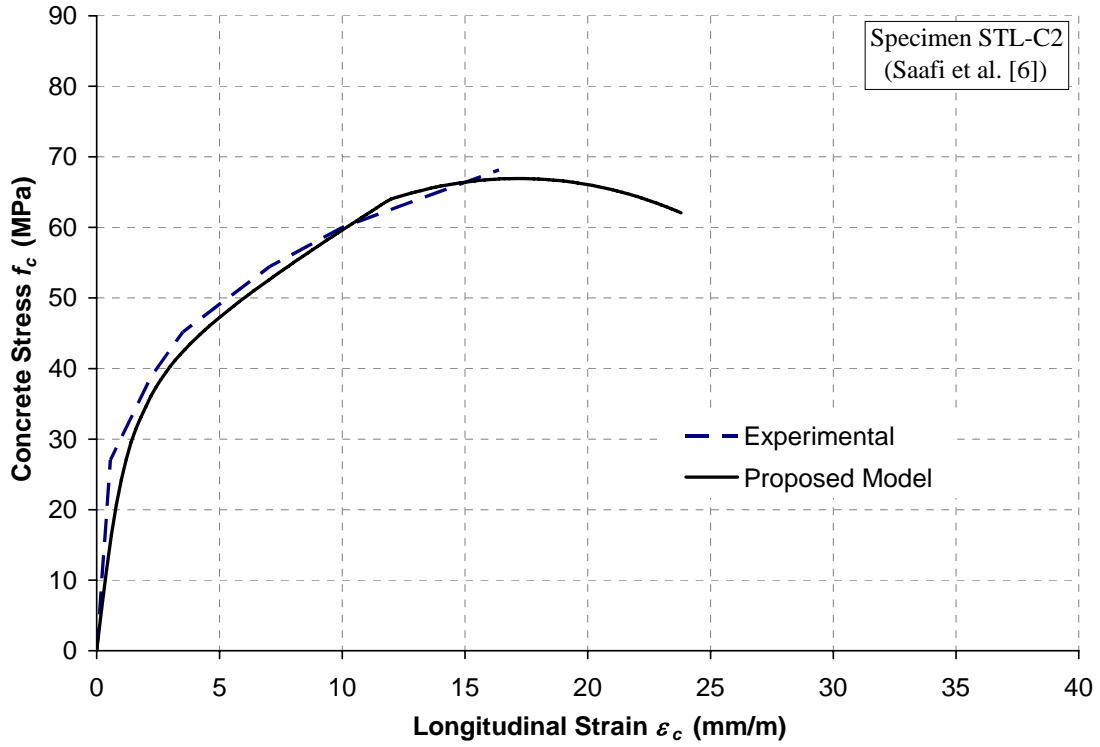


Figure 14: Stress-strain response prediction of proposed model for Specimen STL-C2

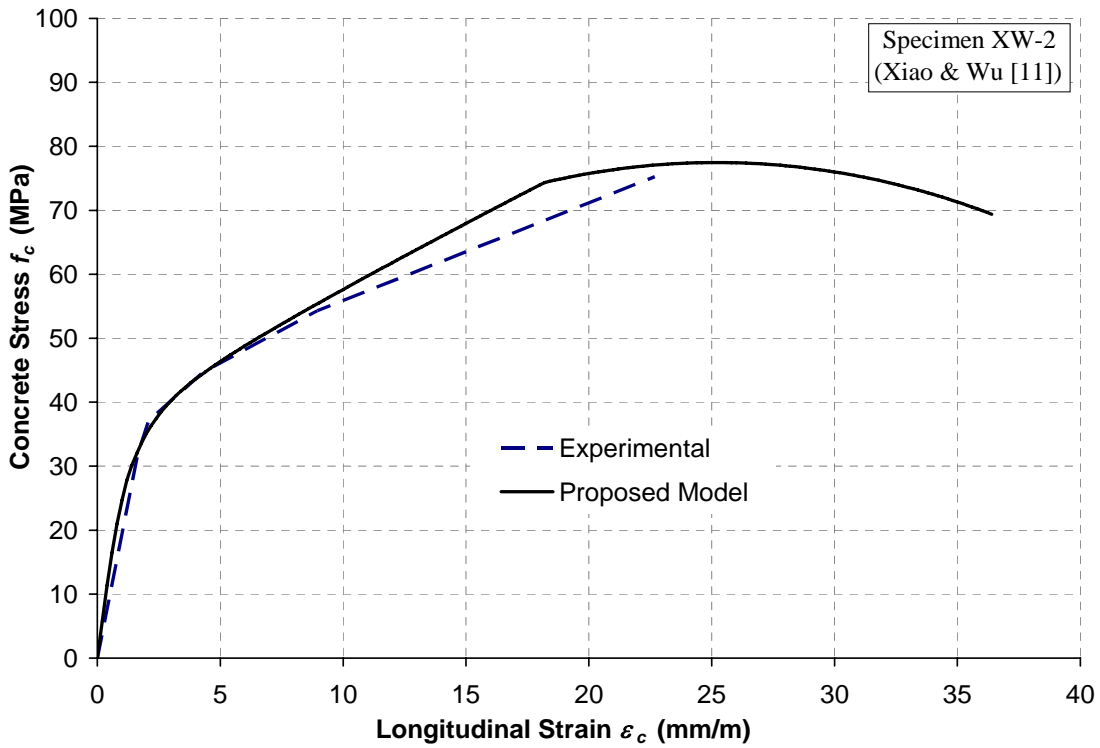


Figure 15: Stress-strain response prediction of proposed model for Specimen XW-2

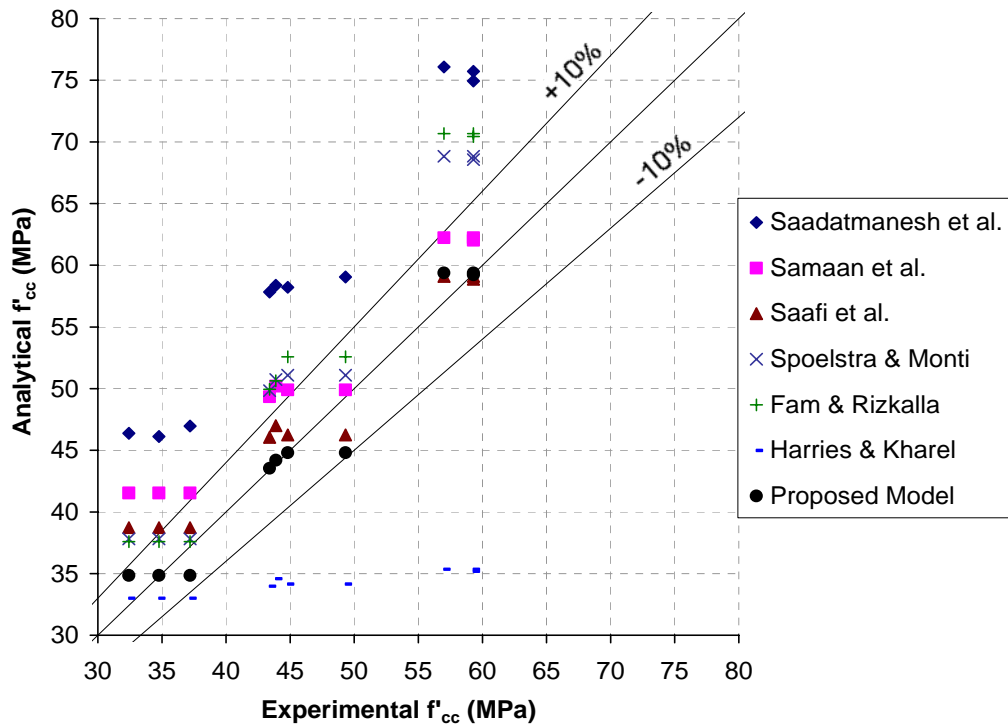


Figure 16: Comparison of all models for prediction of f'_{cc} for Toronto Specimens

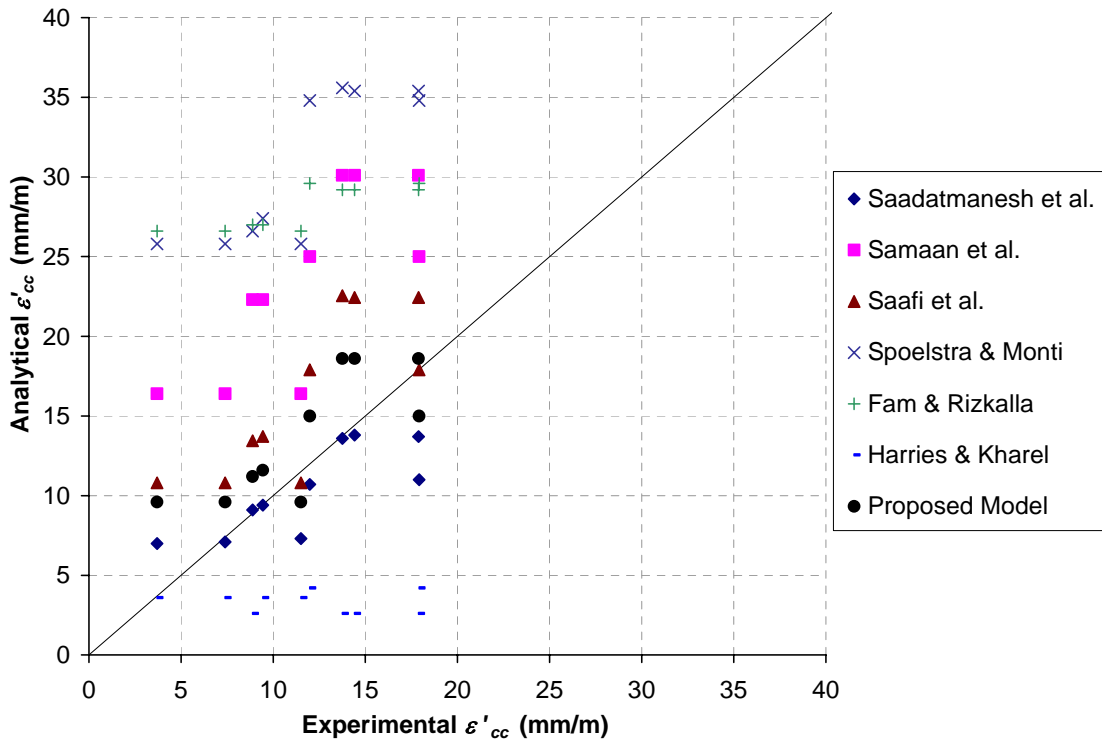


Figure 17: Comparison of all models for prediction of ϵ'_{cc} for Toronto Specimens

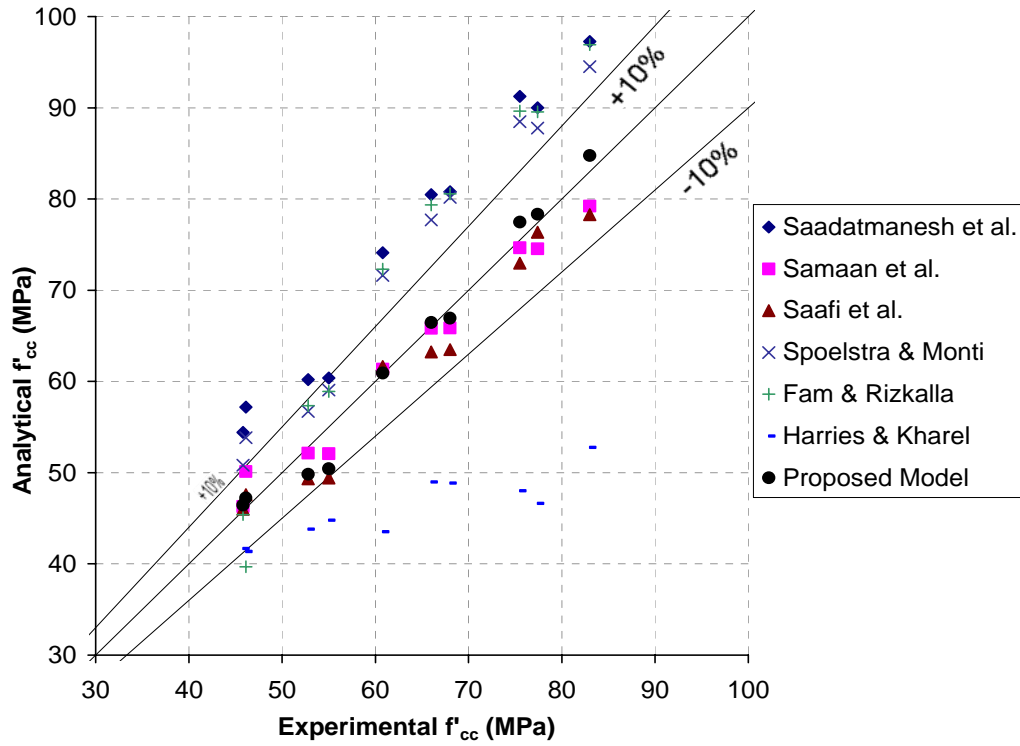


Figure 18: Comparison of all models for prediction of f'_{cc} for Other Specimens

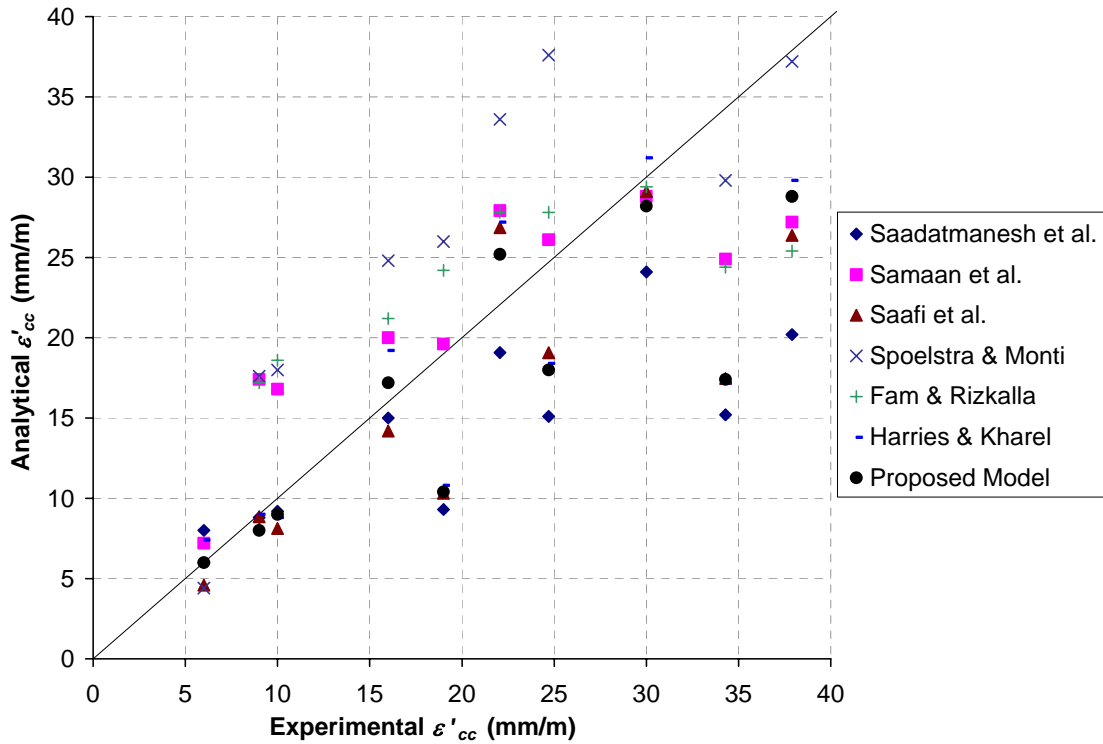


Figure 19: Comparison of all models for prediction of ϵ'_{cc} for Other Specimens